30th International Conference
ENGINEERING MECHANICS 2024
Milovy, Czech Republic, May 14 – 16, 2024

ON DIFFUSION, REACTION, AND FLOW OF HIGH-CONCENTRATION MULTICOMPONENT GAS MIXTURES

Hlavatý T.[*]**, Isoz M.**[**]

Abstract: *Heterogeneous catalysis contributes to producing more than 80 % of all chemical products in the world. Industrial heterogeneous catalysis is a complex process that combines fully three-dimensional mass, momentum, and energy transport on several scales. In the present work, we leverage our previously developed CFD solver for non-isothermal heterogeneously catalyzed reactive flow based on the finite-volume method and extend it with multicomponent Stefan-Maxwell diffusion description to handle high-concetration multicomponent mixtures. The resulting framework is verified and validated on the simple Stefan tube experiment, for which an analytical solution is available.*

Keywords: Stefan-Maxwell diffusion, high concentration reactive flow, OpenFOAM.

1. Introduction

Heterogeneous catalysis plays a crucial role in numerous industrial chemical processes, ranging from mobile applications in catalytic converters for automotive exhaust gas aftertreatment to stationary large industrial reactors for natural gas conversion (Tischer et al., 2001) or ethylene oxychlorination. In the case of mobile catalysts, the active catalytic material is usually coated in the form of a porous layer on the walls of monolith channels (Blažek et al., 2021). For the fixed-bed reactors, the catalyst is deposited on and inside catalyst-carrying particles.

However, there is still significant room for optimization of such processes (Fechete et al., 2012). The efficiency of an arbitrary heterogeneous catalyzed process is strongly dependent on all the transport processes inside the system. In particular, focusing onto mass transport, the following needs to be taken into account, (i) global transport of reactive species inside the reactor, i.e., to and from porous media coated with catalytic material, (ii) local diffusive transport inside the porous structure of the catalyst, and (iii) adsorption of reactants onto active sites and subsequent reaction followed by desorption of products. Furthermore, despite the fact that the proper description of the high-concentration-mixture diffusion, which is common in the real-life industrial processes, is well known for a long time (Taylor and Krishna, 1993), the most of the newly developed computational fluid dynamics (CFD) solvers for coupled momentum and multicomponent mass transfer, e.g. (Chandra et al., 2020), rely on simplified (linear) Fick's diffusion.

The main goal of the present work is to extend our previously developed solver for heterogeneously catalyzed reactive flow (Hlavatý et al., 2023b) by the Stefan-Maxwell diffusion description to deal with the high-concentration mixtures commonly present in the industrial chemical reactors.

2. Model description

The presented model stems from our previously published OpenFOAM solver for the heterogeneously catalyzed reactive flow for the simulations of the catalytic filters in the automotive exhaust gas aftertreatment (Hlavatý et al., 2023b). Non-isothermal reactive flow of an ideal gas in the heterogeneous domain Ω

---

[*] Ing. Tomáš Hlavatý: University of Chemistry and Technology, Technická 5; 166 28, Prague; CZ, and Institute of Thermomechanics, CAS, Dolejškova 1402/5; 182 00, Prague; CZ, hlavaty@it.cas.cz

[**] Ing. Martin Isoz, PhD.: Institute of Thermomechanics, CAS, Dolejškova 1402/5; 182 00, Prague; CZ, isozm@it.cas.cz

doi: 10.21495/em2024-114

is assumed, while the heterogeneity of Ω is ensured by dividing Ω in free space (Ω_{fs}) and porous media (Ω_{pm}), such that $\Omega = \Omega_{\mathrm{fs}} \cup \Omega_{\mathrm{pm}}$ and $\Omega_{\mathrm{fs}} \cap \Omega_{\mathrm{pm}} = \emptyset$, and by using (i) effective diffusion coefficients, and (ii) piece-wise continuous right hand side of governing equations, see (Hlavatý et al., 2022, 2023a,b).

Assuming a Newtonian gas, neglecting heat mechanical sources, and marking the velocity $\boldsymbol{u}$, the mass density ρ, the pressure p, and the temperature T, the steady-state momentum, mass, and heat transfer can be, in order, described by the following set of balances,

$$\nabla \cdot [\rho \boldsymbol{u}\boldsymbol{u}^{\intercal}] - \nabla \cdot [\mu (\nabla \boldsymbol{u} + (\nabla \boldsymbol{u})^{\intercal})] = -\nabla p + \rho \boldsymbol{s}^{\boldsymbol{f}} \,, \tag{1}$$

$$\nabla \cdot (\rho \boldsymbol{u}) = 0 \,, \tag{2}$$

$$\nabla \cdot (\boldsymbol{u} \rho \omega_i) - \nabla \cdot \left(\dot{\boldsymbol{m}}_i^{\mathrm{D}}\right) = s_i^r, \quad i = 1, \ldots, n-1 \,, \tag{3}$$

$$\nabla \cdot (\rho \boldsymbol{u} c_{\mathrm{p}} T) - \nabla \cdot \left(\lambda^{\mathrm{eff}} \nabla T\right) = s^h \,, \tag{4}$$

where μ is the dynamic viscosity of the gas, λ^{eff} is the effective heat conductivity, and c_{p} is the heat capacity. For more information on parameters' computations see (Hlavatý et al., 2023a). The source term $\rho \boldsymbol{s}^{\boldsymbol{f}}$ describes the resistivity of the flow through the porous medium (Ω_{pm}) and is defined based on the Darcy permeability model (Kočí et al., 2019). Reactions are assumed to occur only in the catalytic material, and the chemical-reactions and enthalpy sources are, in order, defined in the form

$$s_i^r = \begin{cases} 0 & \text{in } \Omega_{\mathrm{fs}} \\ \nu_i \varphi_c \, s^r \, M_i & \text{in } \Omega_{\mathrm{pm}} \end{cases} , \quad s^h = \varphi_c \, s^r (-_{\Delta} H_r) \,, \tag{5}$$

where ν_i is the i-th component stoichiometric coefficient, φ_c is the volumetric fraction of the catalyst, and s^r is the reaction rate computed from a rate law considering the local gas temperature and composition.

The gas mass density is assumed to be linked with pressure, and temperature via the ideal gas law $(6)_1$, where R^{g} is the universal gas constant and M^{g} is the composition-dependent molar mass of the gas $(6)_2$, where ω_i, and M_i are the i-th chemical specie mass fraction, and the molar mass, respectively. Supposing a gas mixture of n species, the mass fraction of the n-th component can be expressed using $(6)_3$,

$$\rho = \frac{p\, M^{\mathrm{g}}}{\mathrm{R}^{\mathrm{g}}\, T} \,, \quad M^{\mathrm{g}} = \frac{1}{\sum_{i=1}^{n} \omega_i / M_i} \,, \quad \omega_n = 1 - \sum_{i=1}^{n-1} \omega_i \,. \tag{6}$$

The main contribution of the present work lies in an extension of the specie diffusion mass flux calculation, $\dot{\boldsymbol{m}}_i^{\mathrm{D}}$. In our previous implementations, the diffusive mass flux was computed using Fick's law valid for small concentrations. In the present work, universal Stefan-Maxwell description of the diffusive fluxes is utilized and implemented within the developed solver. Working in the mass-average frame, the Stefan-Maxwell relations can be expressed in a compact matrix form as;

$$\left[\dot{\boldsymbol{m}}^{\mathrm{D}}\right] = \rho \, \left[D^0\right] \, [\nabla \boldsymbol{\omega}] \,, \tag{7}$$

where $\left[\dot{\boldsymbol{m}}^{\mathrm{D}}\right]$ is the matrix of the diffusive mass fluxes of the $(n-1)$ chemical species, i.e. in three spatial dimensions $\left[\dot{\boldsymbol{m}}^{\mathrm{D}}\right] \in \mathbb{R}^{(n-1,3)}$, and $[\nabla \boldsymbol{\omega}]$ is the matrix of the mass fraction gradients, of the same dimension (Taylor and Krishna, 1993). The symbol $\left[D^0\right]$ stands for the $(n-1, n-1)$ dimensional matrix of the multicomponent diffusion coefficients in the mass average frame, which can be calculated as suggested by Taylor and Krishna (1993),

$$\left[D^0\right] = \left[B^{\mathrm{ou}}\right] \, \mathrm{diag}\left(\boldsymbol{\omega}/\boldsymbol{y}\right) \, \left[B^{-1}\right] \, \mathrm{diag}\left(\boldsymbol{y}/\boldsymbol{\omega}\right) \, \left[B^{\mathrm{uo}}\right] \,, \tag{8}$$

where $[B^{\mathrm{ou}}]$, and $[B^{\mathrm{uo}}]$ are mutually inverse matrices of the transformation from the mass to molar average frame and vice versa, respectively. The used form of the transformation matrix is,

$$\left[B^{\mathrm{ou}}\right]_{i,k} = \delta_{i,k} - \omega_i \left(1 - \frac{\omega_n \, y_k}{y_n \, \omega_k}\right), \; i, k = 1, \ldots, n-1 \,, \tag{9}$$

where y_i is the molar fraction of the i-th specie, and $\delta_{i,k}$ is Kronecker delta.

Diagonal matrices $\mathrm{diag}\,(\boldsymbol{\omega}/\boldsymbol{y})_{i,i} = \omega_i/y_i$ and $\mathrm{diag}\,(\boldsymbol{y}/\boldsymbol{\omega})_{i,i} = y_i/\omega_i$ are ratio of the mass (ω) to the molar fraction (y) and vice versa. Finally, the matrix of the diffusion coefficients in the molar average frame $\left[B^{-1}\right]$ is computed as the inversion of the $(n-1, n-1)$ dimensional matrix $[B]$, whose coefficients are defined as follows,

$$[B]_{i,i} = \frac{y_i}{\mathcal{D}_{i,n}} + \sum_{k=1,i\neq k}^{n} \frac{y_k}{\mathcal{D}_{i,k}}\,, \tag{10}$$

$$[B]_{i,j} = -y_i \left(\frac{1}{\mathcal{D}_{i,j}} - \frac{1}{\mathcal{D}_{i,n}}\right). \tag{11}$$

Note that the matrix of the diffusion coefficients $\left[D^0\right]$ is composition-dependent, which means that the Stefan-Maxwell diffusion leads to a non-linear problem.

In general, it is difficult to determine the Stefan-Maxwell binary diffusion coefficients $\mathcal{D}_{i,j}$. However, considering the ideal gas and heterogenous domain, $\Omega = \Omega_{\mathrm{fs}} \cup \Omega_{\mathrm{pm}}$, we can assume that the Stefan-Maxwell binary diffusion coefficients are equal to the effective Fick binary diffusion coefficients, $\mathcal{D}_{i,j} = D^{\mathrm{eff}}_{i,j}$, whose calculation is taken from (Hlavatý et al., 2023a).

3. Numerical results

The new implementation of the diffusive flux was validated on the well known benchmark case of the Stefan tube with the high concentration diffusive mass transfer.

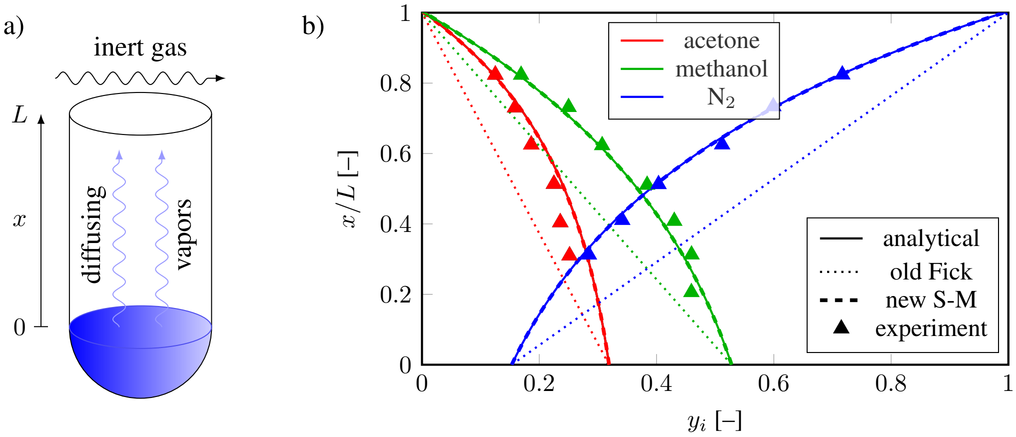

Fig. 1: a) Schematics of the Stefan tube, b) comparison of molar fraction profiles in the Stefan tube computed with different implementations of the custom solver with the experimental data by Carty and Schrodt (1975).

The Stefan tube is a simple device schematically depicted in Fig. 1a. At the bottom of the tube, there is a level of the acetone/methanol mixture. The vapor evaporates and diffuses to the top of the tube. A stream of the inert gas flows across the top of the tube, which keeps the mole fraction of diffusing vapors close to zero there (Taylor and Krishna, 1993). As the diffusion to the top of the tube is a relatively slow process, the change of the liquid level is slow and we can assume a pseudo-steady state. With such an assumption, the boundary conditions for the molar fractions of all the acetone and methanol are Dirichlet and constant,

$$y_i(0) = \frac{p_i^{\mathrm{s}}}{p}\,, \quad y_i(L) = 0\,, \tag{12}$$

where p_i^{s} is the saturated vapor pressure and the system of mass balances (3) can be reduced to the set of the ordinary differential equations with the analytical solution. Furthermore, Carty and Schrodt (1975) published experimental data on the diffusion of acetone/methanol mixture in pure nitrogen. This allowed us to compare new solver concentration profiles (dashed lines) with the analytical solution (solid lines), experiment (triangles), and the old solver implementation (dotted lines) in Fig. 1b.

Let us emphasize three things: (i) the old solver-implementation (old Fick), which assumes constant molar mass of the gas, is not capable resolving cross-diffusion effects occurring in the Stefan tube with a high concentration of the diluted gases, (ii) the new solver-implementation (new S-M) predicts results almost identical to the analytical solution, and (iii) they provide quite good agreement with the experiment.

4. Conclusion

In the present contribution, we delineated fundamental principles of a solver applicable to the simulation of heterogeneously-catalyzed reactive flows. The new solver allows for the simulations of non-diluted reactive mixtures with simultaneous momentum, heat, and mass transfer, while the mass transfer treatment comprises the Stefan-Maxwell approach to multi-component diffusion. For the simplified case of a mass transfer in a Stefan tube, the new solver provides results in a perfect agreement with both the experiment and the available analytical solution. The proposed solver extension allows one to properly describe and optimize complex industrial processes, such as ethylene oxichlorination which is descibed in detail in (Hlavatý et al., 2023a) and illustrated in Fig. 2.

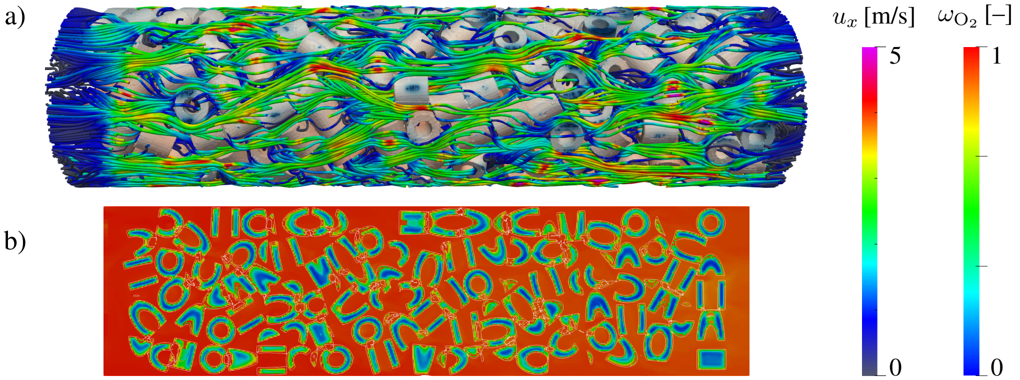

Fig. 2: a) Streamlines colored by streamwise velocity component in industrial packed bed, b) oxygen mass fraction (ω_{O_2}) contours on longitudinal cut through the geometry.

Acknowledgments

The work was financially supported by the institutional support RVO:61388998, by the grant project with No. TN02000069/001N of the Technology Agency of the Czech Republic, and the grant project with No. QL24010110 of the National Agency for Agricultural Research (NAAR).

References

Blažek, M., Žalud, M., Kočí, P., York, A., Schlepütz, C., Stampanoni, M., and Novák, V. (2021) Washcoating of catalytic particulate filters studied by time-resolved X-ray tomography. *Chemical Engineering Journal*, 409, pp. 128057.

Carty, R. and Schrodt, T. (1975) Concentration profiles in ternary gaseous diffusion. *Industrial & Engineering Chemistry Fundamentals*, 14, 3, pp. 276–278.

Chandra, V., Peters, E., and Kuipers, J. (2020) Direct numerical simulation of a non-isothermal non-adiabatic packed bed reactor. *Chemical Engineering Journal*, 385, pp. 123641.

Fechete, I., Wang, Y., and Védrine, J. C. (2012) The past, present and future of heterogeneous catalysis. *Catalysis Today*, 189, 1, pp. 2–27.

Hlavatý, T., Isoz, M., and Khýr, M. (2023a) Simulation of heterogeneously-catalyzed non-isothermal reactive flow in industrial packed beds. pp. 44–51.

Hlavatý, T., Isoz, M., and Kočí, P. (2022) Developing a coupled cfd solver for mass, momentum and heat transport in catalytic filters. pp. 79–86.

Hlavatý, T., Kočí, P., Isoz, M., Deka, D., and Partridge, W. (2023b) Balanced fast-spacims capillary configurations provide practically noninvasive channel-average measurements in catalytic monoliths. *Chemical Engineering Science*, 282, pp. 119272.

Kočí, P., Isoz, M., Plachá, M., Arvajová, A., Václavík, M., Svoboda, M., Price, E., Novák, V., and Thompsett, D. (2019) 3D reconstruction and pore-scale modeling of coated catalytic filters for automotive exhaust gas aftertreatment. *Catalysis Today*, 320, pp. 165–174.

Taylor, R. and Krishna, R. (1993) *Multicomponent mass transfer*, 2. John Wiley & Sons.

Tischer, S., Correa, C., and Deutschmann, O. (2001) Transient three-dimensional simulations of a catalytic combustion monolith using detailed models for heterogeneous and homogeneous reactions and transport phenomena. *Catalysis Today*, 69, 1, pp. 57–62.